

LIMITS ON GPS CARRIER-PHASE TIME TRANSFER*

M. A. Weiss

National Institute of Standards and Technology

Time and Frequency Division, 325 Broadway Boulder, Colorado, USA

Tel: 303-497-3261, Fax: 303-497-6461, E-mail: mweiss@boulder.nist.gov

Abstract

The stability of differential delays between Global Navigation Satellite receivers is critical for time and frequency transfer. We study the limit of this transfer between two specific receivers due to effects in data taken from these receivers while they were connected with a splitter to the same antenna for 128 days. We show that the C/A-to-P1 TDEV stability is consistent with a flicker PM model at about 10 ps from 1 d – 10 d. The TDEV stability of differential code shows models of flicker PM at under 50 ps for C/A code, and white PM starting at under 100 ps at 1 d for P2 code. P3 code transfer would perhaps be limited by receiver variations to about 400 ps flicker PM. Carrier-only transfer shows a rate offset of $+2 \times 10^{-16}$ for L1 and -2×10^{-16} for L2. Thus, a carrier-only frequency transfer technique would be limited to 8×10^{-16} for the ionosphere-free combination.

INTRODUCTION

For the comparison of clocks using signals of Global Navigation Satellite Systems (GNSS) such as the Global Positioning System (GPS) [1] satellites, the total delay through the receiver and antenna system is critical. It is impossible to tell the difference between a change in this delay and the changes due to the clock referencing the receiver when comparing to a remote clock. To determine the relative stability of two receivers, we connected them through a splitter to the same antenna and cable, as well as referencing the receivers with the same clock. One receiver, NISA, was in a temperature-controlled chamber. The other, NISV, was in the same room, but not otherwise temperature-controlled. We mention the manufacturers for information only. No implication of endorsement or criticism is implied. The NISA receiver was an Ashtech Z12T. The NISV receiver was a NovAtel T-Sync receiver, with an OEM4 board.

A separate issue for time transfer is that some receivers, such as the NovAtel T-Sync receiver, do not track the P1 code, but only the C/A (also known as C1) code. Though the P-code has a 10.23 MHz chip rate, versus the 1.023 chip rate of the C1 code, the signal-to-noise ratio is about the same for locking the signals, particularly with the codeless technique used for P1 with non-authorized receivers. Hence, the sharpness of the code lock is the same for both. Multi-path techniques can narrow the tracking bandwidth just as much for both signals. However, ephemeris and clock data of the International GNSS Service (IGS) reference the P1 phase-time on the satellite [2]. Hence, processing should apply the C1-P1 differences. We report these values to show the magnitude of this effect.

* Contribution of U.S. government, not subject to copyright.

The difference between the code and carrier data reflects the limits on GPS time and frequency transfer. Because the receivers used the same antenna, the code and carrier phase can be differenced directly without any geodetic processing software. Comparison of code phases was direct. Comparison of carrier phases required the removal of an arbitrary constant from the beginning of each satellite pass. We report the differential measurements between the receivers for each of these signal types without using geodetic processing software.

ANALYSIS TECHNIQUE

The geodetic-type GPS receivers were connected with a splitter to the same antenna for 128 days. RINEX [2] files were stored with points taken every 30 seconds. Measurements were stored for the L1 and L2 carrier phases, as well as the C1, P1, and P2 code phases. These data were used to obtain the C1-P1 values for one receiver, as well as continuous averages of the differential delay through the two receivers for each of the four data types.

The C1-P1 data were differenced for each satellite at each reference time. These differences were then averaged across all satellites available at each time. The Time Deviations (TDEV) of these data were computed [3].

Changes in the receiver differential delays were determined for the two codes in common, C1 and P2, and for the L1 and L2 carrier phases. For the code data, we found the average of the differences over all satellites tracked by both receivers at all available reference times. This process gave the changes in receiver delay for each of the codes studied, C1 and P2, modulo uncertainties in the reference signal differences.

The processing of the carrier data was not as simple because the data were complicated by the differential cycle ambiguity between the two receivers. To account for this uncertainty, a constant was removed from each differenced datum in a satellite's pass before calculating the average. The constant was the first datum in the pass minus the current existing average. This entailed one constant per pass for every satellite for each of the L1 and L2 carrier phases.

RESULTS

Fig. 1 shows the average C1 to P1 difference over all satellites tracked over the 180 days, with TDEV of these data in Fig. 2. The mean is -0.414 ns. The noise type is consistent with a white phase modulation (PM) model in short term, with a level of 225 ps at 30 s. There is a diurnal variation of about 70 ps, dropping to about 20 ps at 1 d, with a flicker PM performance at the 10 ps level thereafter. Individual satellites have values approaching 1.0 ns at 30 s with performance as white PM. Since the number of satellites averaged about 9, these values are consistent.

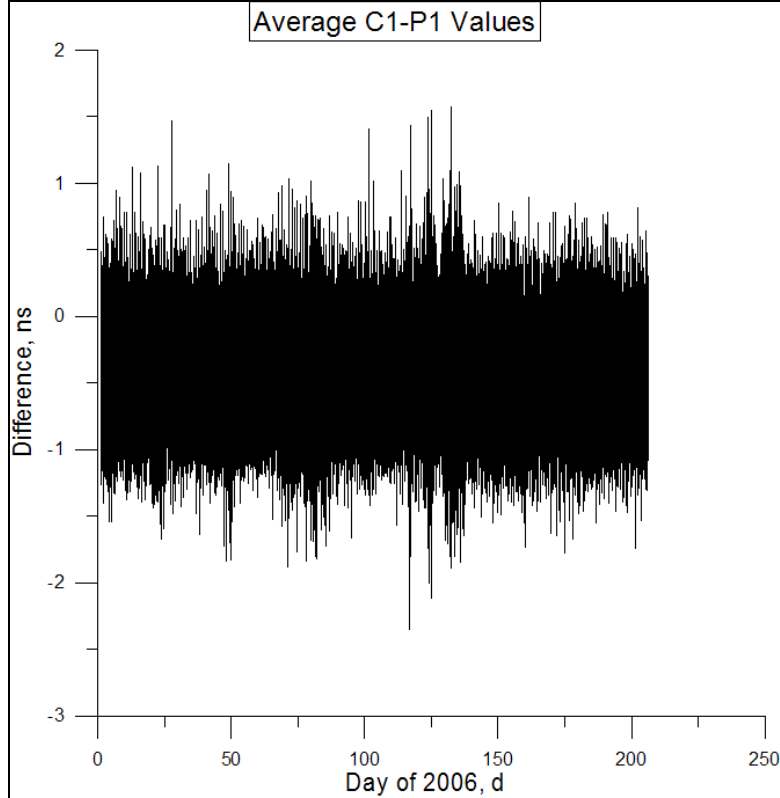


Figure 1. C1-P1 values averaged over typically nine satellites. The mean was -0.414 ns.

Fig. 3 shows the result of the analysis done on the L1 carrier data. It shows the change in differential delay over time between the two receivers. These results show that the differential delay increased from zero as time progressed, with some apparent linearity, though with sudden steps in some places. Analyzing the L2 carrier data yielded similar results, as in Fig. 4, though with the differential delay decreasing. There appears to be an underlying linear change in phase delay between the two receivers of order 2 ns in 100 d, increasing for L1 and decreasing for L2 data. Some of this may be due to the random-walk process. TDEV as in Fig. 5 and 6 at 10 d is about 100 ps. The expected phase deviation would be $\sqrt{3}$ times the TDEV values, continuing to increase by the square root of the averaging time out to the data length. With the data length of order 100 d, we multiply 100 ps times $\sqrt{3}$ twice and obtain about 300 ps as potentially due to random-walk phase modulation (RWPM).

It would be convenient to blame the increase in offset on a random-walk process. However, it looks perhaps too linear for this. The approximate 2 ns change over 100 d, increasing with L1 data, yet decreasing with L2, corresponds to an error in frequency transfer of about 2×10^{-16} for each carrier. This error would not enter into a transfer technique that used the code to estimate the cycle ambiguity of the carrier. If a true carrier-only technique is used, with the ionosphere-free combination of $2.5 \times L1 + 1.5 \times L2$, the frequency transfer error due to this underlying drift in the receiver carriers would be 8×10^{-16} . This would be a significant effect when using GPS carrier-phase techniques to compare frequency standards whose uncertainties are below 1×10^{-15} . There is some evidence that an effect like this may have been seen before in a comparison to Two-Way Satellite Time and Frequency Transfer [4].

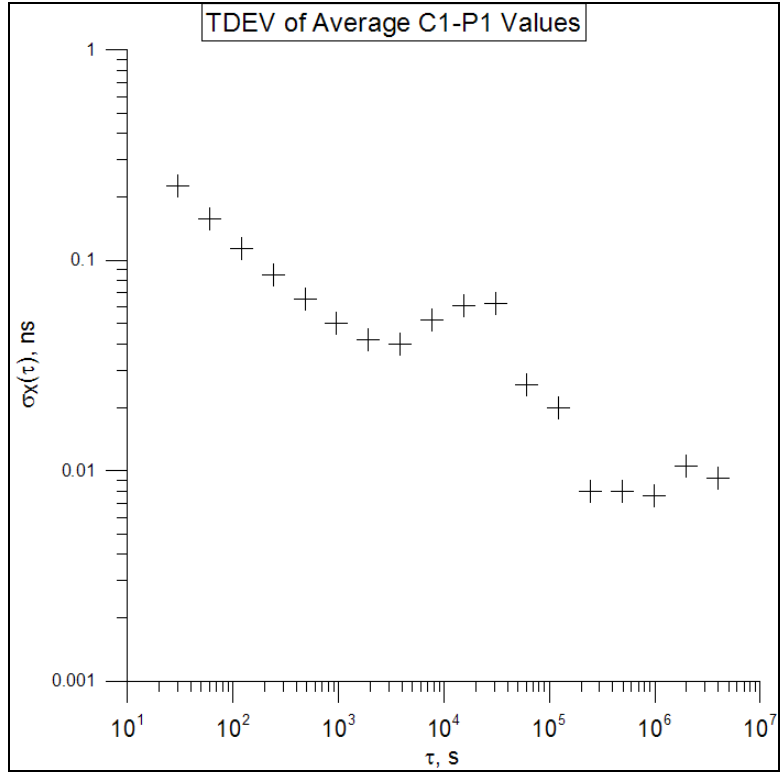


Figure 2. TDEV of the values in Fig. 1. The short term of 225 ps at 30 s is consistent with a white PM model. A diurnal variation at about 70 ps drops to a flicker PM floor at about 10 ps.

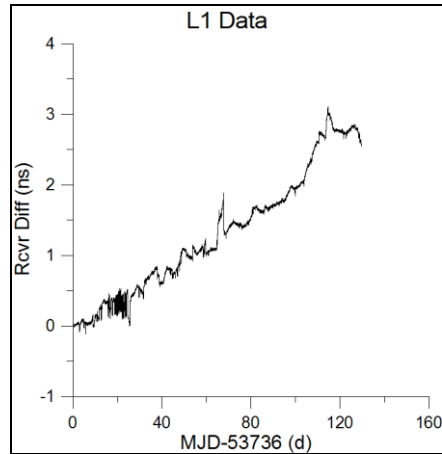


Figure 3. Plot of the changes in differential delay through the two receivers for the GPS carrier L1. The delay is measured in nanoseconds and is plotted against the day of year 2006, by subtracting the Modified Julian Day (MJD) 54736. The data cover a 128-day period.

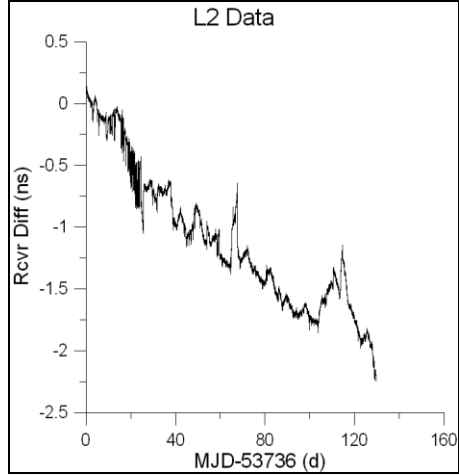


Figure 4. Plot of the changes in differential delay through the two receivers for the GPS carrier L2. The delay is measured in nanoseconds and is plotted against the day of year 2006, by subtracting the Modified Julian Day (MJD) 54736. The data cover a 128-day period.

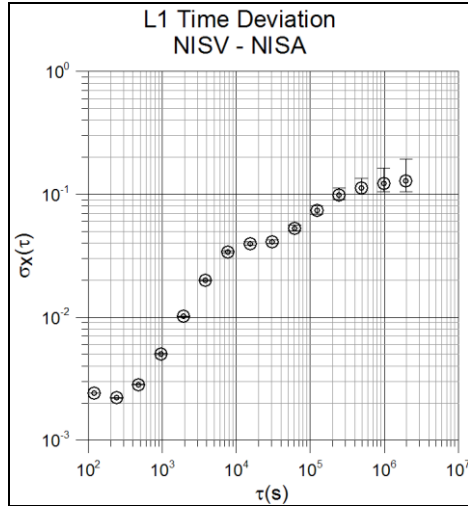


Figure 5. Plot of the Time Deviation of the L1 averaged NISV-NISA data.

The offsets we found represent differential delays between the two receivers. The possible causes of this, as mentioned above, include: the RWPM, the different response to multi-path interference between the receivers, the fact that we calibrate the pass generally when the satellite is at a low angle, and finally a true change in delay between the receivers. Given that one receiver is temperature-controlled, this delay change might be a temperature coefficient between the receivers.

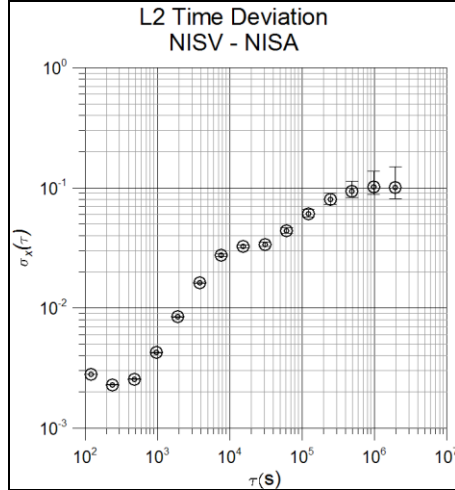


Figure 6. Plot of the Time Deviation of the L2 averaged NISV-NISA data.

Fig. 7 shows the results of the differential delay computed for the C1 code data. The P2 code data results can be seen in Fig. 8. The outcome here did not show ramps as for the carrier data, as can be seen more clearly in Fig. 9 and Fig. 10, where we have low-pass filtered the data using a Kalman smoother. There are somewhat positive changes for C1 and generally negative for P2, over the period of study, but the magnitudes are much smaller. The effects do not appear to be linear. C1 appears to have jumps of about 0.2 ns over a few days. P2 seems to wander negative of order -0.1 ns over 100 d. Thus, this evidence suggests that a GPS carrier-phase time transfer technique should use the code to resolve carrier ambiguity. While there may be some changes in delay occasionally that might be problematic, there is no evidence here of an ongoing systematic that would impact frequency transfer at a level of a few parts in 10^{16} . Perhaps the carrier could be used to smooth possible code steps.

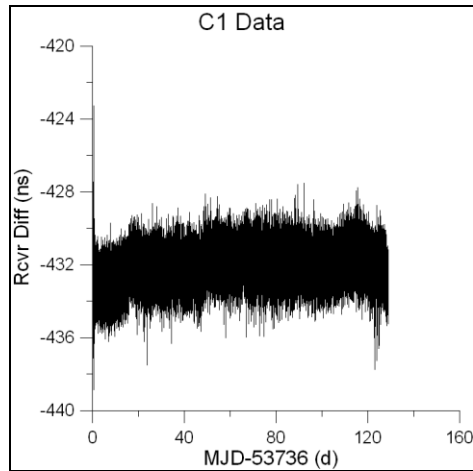


Figure 7. Plot of the changes in differential delay through the two receivers for the GPS code C1. The delay is measured in nanoseconds and is plotted against the day of year 2006, by subtracting the Modified Julian Day (MJD) 54736. The data cover a 128-day period.

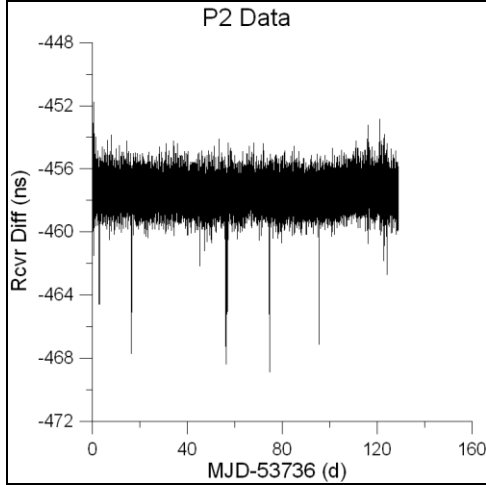


Figure 8. Plot of the changes in differential delay through the two receivers for the GPS code P2. The delay is measured in nanoseconds and is plotted against the day of year 2006, by subtracting the Modified Julian Day (MJD) 54736. The data cover a 128-day period.

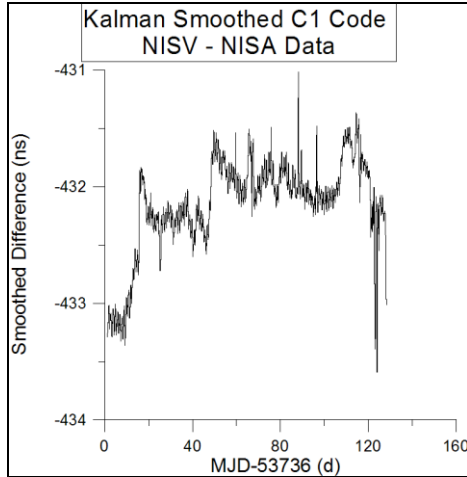


Figure 9. Plot of the Kalman Smoothed C1 code averaged data, showing the lack of slope as in the L1 carrier phase data.

The TDEV values for the codes are shown in Fig. 11 and Fig. 12 for the C1 and P2 data, respectively. They start with the integration time of 120 s, since we averaged four points to reduce the processing load. The short-term noise is consistent with a White PM model. The P2 level of 160 ps at 120 s is slightly better than the C1 level of 200 ps at 120 s, perhaps because of the higher chipping rate. However, the diurnal variation is somewhat worse for the P2. C1 has a TDEV of 40 ps at the almost half-day peak, whereas the P2 level is 120 ps. They both drop below 100 ps at 1 day, however.

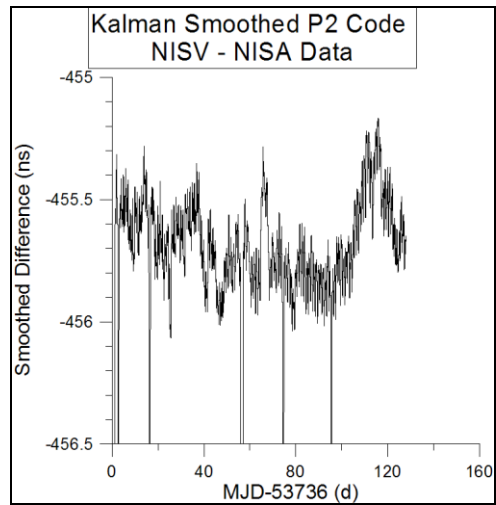


Figure 10. Plot of the Kalman Smoothed P2 averaged data, showing the lack of slope as in the L2 data. The plot is clipped with a minimum of -456.5 ns due to some apparently bad data.

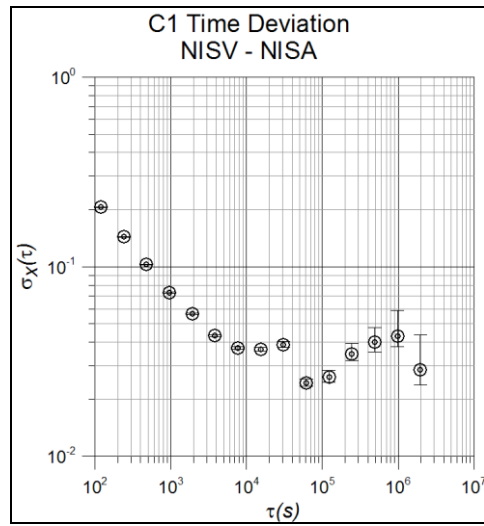


Figure 11. Plot of the Time Deviation of the C1 averaged data.

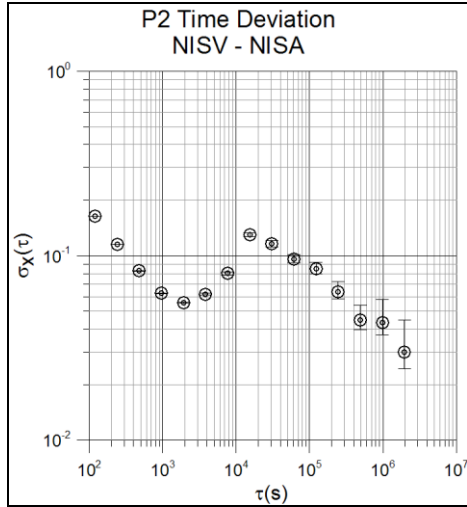


Figure 12. Plot of the Time Deviation of the P2 averaged data.

CONCLUSIONS

The C1 to P1 differences for individual satellites approach 1.0 ns at 30 s, though when averaged across all available satellites (typically 9), this drops to 225 ps. These values average down as white PM, until they rise with a diurnal variation of about 70 ps. After dropping to 20 ps at 1 d, they further drop to a flicker PM floor of 10 ps.

We also studied the differential delays between two GPS geodetic receivers at NIST of different manufacture, NISV and NISA. We looked at the difference between the receivers' time stamps of the C1 and P2 codes, and the L1 and L2 phases. The differences between receiver times for the L1 and L2 phases changed in an apparent almost linear way by 2 ns over 100 d, with the L1 data increasing and the L2 data decreasing. This implies a potential limit in frequency transfer for a carrier-only GPS carrier frequency transfer of 8×10^{-16} for the ionosphere-free combination. The C1 and P2 code differences exhibit no such linear trend. However, there are some jumps in the C1 averages of 0.2 ns over a few days, and some outliers in the P2 data.

REFERENCES

- [1] B. W. Parkinson and J. J. Spilker, Jr., 1996, **Global Positioning System: Theory and Applications** (American Institute of Aeronautics and Astronautics, Washington, D.C.).
- [2] W. Gurtner and G. M. Mader, "The RINEX format: current status, future developments," <http://www.navcen.uscg.gov/pubs/gps/rinex/default.htm>
- [3] D. W. Allan, M. A. Weiss, and J. L. Jespersen, 1991, "A Frequency-Domain View of Time-Domain Characterization of Clocks and Time and Frequency Distribution Systems," in Proceedings of the 1991 IEEE Symposium on Frequency Control, 29-31 May 1991, Los Angeles, California, USA (IEEE 91CH2965-2), pp. 667-678.

- [4] T. E. Parker, V. S. Zhang, A. McKinley, L. M. Nelson, J. Rohde, and D. Matsakis, 2003, “Investigation of Instabilities in Two-Way Satellite Time and Frequency Transfer,” in Proceedings of the 34th Annual Precise Time and Time Interval (PTTI) Systems and Applications Meeting, 3-5 December 2002, Reston, Virginia, USA (U.S. Naval Observatory, Washington, D.C), pp. 381-390.